Kathmandu University
Journal of Science, Engineering and Technology

Siddalinga & Shashikala, Vol. 12, No. I, June, 2016, pp 49-62.

ORIGINAL RESEARCH ARTICLE OPEN ACCESS

FREE CONVECTIVE FLOW OF A COUPLE STRESS FLUID THROUGH A VERTICAL POROUS CHANNEL IN THE PRESENCE OF A TRANSVERSE MAGNETIC FIELD

[1]Siddalinga Prasad M.[*], [2]Shashikala B. S.
[1]Department of Mathematics, Siddaganga Institute of Technology, Tumkur, Karnataka, India
[2]Department of Mathematics, Government SKSJIT, Bangalore, Karnataka, India

*Corresponding author's e-mail: msp_maths@rediffmail.com
Received 22 March, 2016; Revised 10 May, 2016

ABSTRACT

Nonlinear oberbeck convection of a couple stress fluid in a vertical porous channel in the presence of transverse magnetic field is investigated in this paper. Analytical solution is obtained using the perturbation technique for vanishing values of the buoyancy parameter. Numerical solution of the nonlinear governing equations is obtained using the finite difference technique to validate the results obtained from the analytical solutions. The influence of the physical parameters on the flow, such as couple stress parameter, Hartmann number, temperature parameter, porous parameter and buoyancy parameter are evaluated and presented graphically. A new approach is used to analyse the flow for strong, weak and comparable porosity cases. It is found that increase in porous parameter, couple stress parameter, Hartmann number and temperature parameters decrease the velocity considerably.

Keywords: Couple stress parameter, Vertical porous channel, Magnetic field, Finite difference technique, Perturbation technique.

INTRODUCTION

Natural convection in a vertical channel has been the focus of investigation for a long time because of its practical applications such as cooling of electronic equipment, passive heating in solar collectors, ventilation of buildings and heat removal in nuclear science applications. Elenbaas [1] studied theoretical and experimental analysis of natural convection between two isothermal parallel plates. He intends at the optimization of heat transfer rate. Bodoia and Osterle [2] studied numerically the development of free convection boundary layer between parallel isothermal vertical plates using finite difference method. Their studies concerned with variation in temperature, pressure and velocity throughout the flow field. Aung et Al. [3] have conducted experimental and numerical studies on the evolution of laminar free convection between vertical plates with asymmetric heating, under the thermal boundary conditions of uniform heat flux and uniform wall temperature. Since then a number of studies have been reported in the literature with focus concentrated on the problem of free convection heat transfer and fluid flow between vertical parallel plates.

The study of non-Newtonian fluids has attracted many researchers because of their applications in engineering and industry, particularly in the extraction of crude oil from petroleum products, solidification of liquid crystals, cooling of metallic plate in a bath to name a few. Different models have been proposed to explain the behaviour of non-Newtonian fluids (Aero *et. al.*, [4], Eringen, [5], Stokes, [6]). Among these couple stress introduced by Stokes [6] has distinct features, such as

Kathmandu University
Journal of Science, Engineering and Technology

Siddalinga & Shashikala, Vol. 12, No. I, June, 2016, pp 49-62.

presence of couple stresses, body couples and non-symmetric stress tensor. Couple stress fluid theory presents models for fluids whose microstructure is of mechanical significance. The effect of very small micro-structure can be felt if the characteristic geometric dimension of the problem is of the same order of magnitude as the size of the microstructure. Thus the main feature of couple stresses is to introduce a size dependent effect.

Umavathi and Malashetty [7] have studied the convection in a couple stress fluid through a porous media in a vertical channel. They have concluded that the effect of couple stress parameter is to reduce the velocity. Maen Al Rashdan *et. al.* [8] have studied heat and mass transfer through porous media with chemical reaction in a micropolar fluid. They have shown that the micropolar fluid parameter suppress the velocity where as it increases the micro-rotation velocity. Tomer *et. al.*, [9] have studied the effect of variable viscosity along an inclined plate with an applied magnetic field. They have shown that velocity and temperature increase with variable viscosity. Rudraiah and Shashikala [10] have studied the effect of electric field in vertical channel filled with poorly conducting liquid. They have shown that effect of electric field is to decrease the velocity and temperature of the fluid. Later, Srinivasacharya and Kaladhar [11] have studied the hall and ion slip effects on fully developed electrically conducting couple stress fluid flow between vertical parallel plates in the presence of a temperature dependent heat source. It is concluded that the effect of couple stresses in the fluid decreases the velocity and temperature. Recently Rudraiah *et. al.* [12] have studied Oberbeck convection in a chiral fluid through porous media with an external constraint of magnetic field. They have concluded that electromagnetic thermal number augments the fluid velocity and temperature.

Most of these studies deal with either Newtonian or non-Newtonian fluid flows in the absence of magnetic field. It is desirable to study the effect of transverse magnetic field on vertical porous layer of a couple stress fluid. An attempt is made to analyse a fully developed couple stress fluid in a vertical channel in order to know the nature of flow for sparse, comparable and dense porous medium with respect to couple stresses in the fluid and an applied magnetic field.

To achieve the above objective, the required basic equations and boundary conditions are given in section 2. Analytical and numerical solutions are derived in section 3. The skin friction, Rate of heat transfer and Mass flow rate are given in section 4, results and discussion in section 5 and general conclusions are drawn in final section.

MATHEMATICAL FORMULATION

We consider the flow of Boussinesq couple stress fluid in a vertical porous channel bounded between two infinite walls as shown in Fig.1. It is assumed that the fluid possesses constant properties expect for density. We assume that the density variation due to temperature differences is used only to express the body force term as buoyancy term. The x- axis is taken along the walls and the y-axis perpendicular to it. The walls are placed at a distance 2b apart and maintained at constant temperatures T_1 and T_2. The fluid is free form external couples. Since the boundaries are infinite along the x-direction, the physical quantities namely velocity and temperature depend only on the y co-ordinate. A uniform transverse magnetic field of strength B_0 is applied in the direction perpendicular to the flow.

Kathmandu University
Journal of Science, Engineering and Technology

Siddalinga & Shashikala, Vol. 12, No. I, June, 2016, pp 49-62.

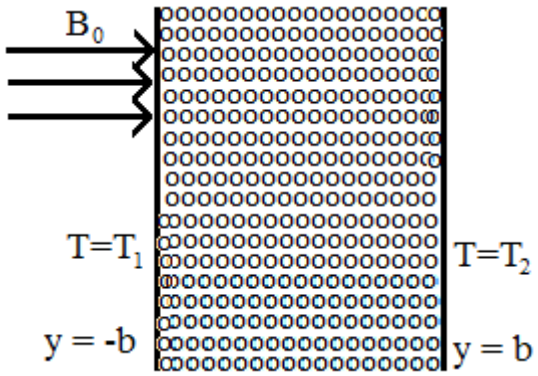

Figure 1: Physical Configuration

The basic equations for the couple stress flow through a porous media in the presence of external constrain of magnetic field for a fully developed flow are

$$\frac{\eta}{\mu}\frac{d^4u}{dy^4}-\frac{d^2u}{dy^2}-\frac{g\beta\left(T-T_0\right)}{\upsilon}+\left(\frac{\sigma B_0{}^2}{\mu}+\frac{1}{K_0}\right)u=0\,, \qquad (2.1)$$

$$\frac{d^2T}{dy^2}+\frac{\rho_0\upsilon}{K_c}\left(\frac{du}{dy}\right)^2=0\,, \qquad (2.2)$$

$$\rho=\rho_0\left[1-\beta\left(T-T_0\right)\right], \qquad (2.3)$$

subject to boundary conditions

$$u=\frac{d^2u}{dy^2}=0 \quad at \quad y=\pm b\,, \qquad (2.4)$$

$$T=T_1 \quad at \quad y=b\,, \qquad (2.5)$$

$$T=T_2 \quad at \quad y=-b\,, \qquad (2.6)$$

where η material constant, μ fluid viscosity, β coefficient of thermal expansion, ρ density, ρ_0 reference density, υ kinematic viscosity, σ porous parameter, g acceleration due to gravity, u velocity of the fluid along x-direction, K_c thermal conductivity, T temperature, K_0 is the permeability of the porous medium.

Boundary conditions on velocity represent the no-slip conditions at the solid boundaries and that of the temperature is that the plates are isothermally maintained at different temperatures T_2 and T_1 ($T_2 > T_1$).

We make the Eqs. (2.1) – (2.6) dimensionless by introducing the non-dimensional variables

$$y^*=\frac{y}{b}, \theta^*=\frac{T-T_0}{T_1-T_0}, u^*=\frac{\upsilon}{g\beta b^2\left(T_1-T_0\right)}u \qquad (2.7)$$

Eqs. (2.1) and (2.6) (after neglecting the asterisk) become

Kathmandu University
Journal of Science, Engineering and Technology

Siddalinga & Shashikala, Vol. 12, No. I, June, 2016, pp 49-62.

$$k\frac{d^4u}{dy^4}-\frac{d^2u}{dy^2}+\ell^2u=\theta, \tag{2.8}$$

$$\frac{d^2\theta}{dy^2}+N\left(\frac{du}{dy}\right)^2=0, \tag{2.9}$$

subject to boundary conditions

$$u=\frac{d^2u}{dy^2}=0 \quad at \quad y=\pm 1, \tag{2.10}$$

$$\theta=1 \quad at \quad y=1, \tag{2.11}$$

$$\theta=1+m \quad at \quad y=-1, \tag{2.12}$$

where

$\ell^2=M^2+\sigma^2$ is a dimensionless group, $M^2=\frac{\sigma B_0{}^2b^2}{\rho\upsilon}$ is the Hartmann number.

$\sigma=\frac{b}{\sqrt{K_0}}$ is the porous parameter, $k=\frac{\eta}{\mu b^2}$ is the couple stress parameter.

$N=\frac{\rho_0 g^2 b^4\left(T_1-T_0\right)}{\rho K_c}$ is the buoyancy parameter and m the temperature parameter.

METHOD OF SOLUTION:

Equations (2.8) and (2.9) constitute a boundary value problem which is coupled non-linear equations because of viscous dissipation term and hence it is difficult to get closed form solutions analytically in general. Therefore, we find the analytical solution for the particular case and the numerical solution for the general case.

1. Analytical Solution:

Coupled non-linear equations are not amenable for analytical solution in general, however for vanishing buoyancy parameter, N, Eqs. (2.8) and (2.9) become linear and can be solved exactly. Vanishing of N will lead to neglecting viscous dissipation. The value of N also indicates the state of the plates, N<0 corresponds to the absence of convection currents. However, small N suggests the use of perturbation technique to solve these coupled nonlinear equations. Accordingly, we write

$$(u,\theta)=(u_0,\theta_0)+N(u_1,\theta_1)+N^2(u_2,\theta_2)+..... \tag{3.1.1}$$

where u_0 and θ_0 are the values of u and θ at N=0 and remaining terms of first and higher order give a correction to u_0 and θ_0 which accounts for the dissipative effects.

Substituting Eq. (3.1.1) in to Eqs. (2.8) and (2.9) and equating the like powers of N to zero, we get Zeroth order equations:

$$\frac{d^2\theta_0}{dy^2}=0 \tag{3.1.2}$$

Kathmandu University
Journal of Science, Engineering and Technology

Siddalinga & Shashikala, Vol. 12, No. I, June, 2016, pp 49-62.

$$k\frac{d^4u_0}{dy^4}-\frac{d^2u_0}{dy^2}+\ell^2u_0=\theta_0 \tag{3.1.3}$$

First order equations:

$$\frac{d^2\theta_1}{dy^2}=-\left(\frac{du_0}{dy}\right)^2 \tag{3.1.4}$$

$$k\frac{d^4u_1}{dy^4}-\frac{d^2u_1}{dy^2}+\ell^2u_1=\theta_1 \tag{3.1.5}$$

The corresponding boundary conditions are

$$u_0=\frac{d^2u_0}{dy^2}=0 \quad at \quad y=\pm1 \tag{3.1.6}$$

$$\theta_0=1 \quad at \quad y=1 \tag{3.1.7}$$

$$\theta_0=1+m \quad at \quad y=-1 \tag{3.1.8}$$

$$u_1=\frac{d^2u_1}{dy^2}=0 \quad at \quad y=\pm1 \tag{3.1.9}$$

$$\theta_1=0 \quad at \quad y=\pm1 \tag{3.1.10}$$

Equations (3.1.2) – (3.1.5) are solved analytically for three possible cases namely sparsely packed, densely packed and thickly packed porous media depending on the sign of the discriminant of the auxiliary equation of the differential equation (3.1.3). Practically these results are of immense use as they will highlight mathematically the relationship between permeability, magnetic field and couple stress parameter. Stokes [6] has shown that the effect of couple stresses is quite large for small values of $k=\frac{\bar{\ell}}{b}$ where b is a typical dimension of the flow geometry and $\bar{\ell}=\sqrt{\mu\eta}$ is the material constant. If $\bar{\ell}$ is a function of the molecular dimension of the liquid, then it will vary greatly for different liquids. Hence, this analysis is also helpful to choose the appropriate liquid depending on the nature of the porous material.

The solution of the Eq. (3.1.2) on using Eqs. (3.1.7) - (3.1.8) is

$$\theta_0=1+\frac{m}{2}(1-y) \tag{3.1.11}$$

The solution of Eqs. (3.1.3) to (3.1.5) on using Eqs. (3.1.6), (3.1.9), (3.1.10) and (3.1.11) are given in the following section for sparse porosity, comparable porosity and dense porosity cases.

Case (i): Sparse porosity (i.e. $4k\ell^2<1$)

$$u_0=\bar{A}_1\cosh p_1y+\bar{A}_2\sinh p_1y+\bar{A}_3\cosh p_2y+\bar{A}_4\sinh p_2y+\frac{1}{\ell^2}-\frac{m(1-y)}{2\ell^2}, \tag{3.1.12}$$

Kathmandu University
Journal of Science, Engineering and Technology

Siddalinga & Shashikala, Vol. 12, No. I, June, 2016, pp 49-62.

where $p_1 = \sqrt{\frac{1+\sqrt{1-4k\ell^2}}{2k}}$, $p_2 = \sqrt{\frac{1-\sqrt{1-4k\ell^2}}{2k}}$ are real numbers and the coefficients in Eq. (3.1.12) are computed using Cramer's rule i.e., $\bar{A}_i = \frac{\Delta_i}{\Delta}$,

$$\Delta = \begin{bmatrix} Chp_1 & Shp_1 & Chp_2 & Shp_2 \\ Chp_1 & -Shp_1 & Chp_2 & -Shp_2 \\ p_1^2 Chp_1 & p_1^2 Shp_1 & p_2^2 Chp_2 & p_2^2 Shp_2 \\ p_1^2 Chp_1 & -p_1^2 Shp_1 & p_2^2 Chp_2 & -p_2^2 Shp_2 \end{bmatrix}, \quad R = \frac{-1}{\ell^2}\begin{bmatrix} 1 \\ 1-m \\ 0 \\ 0 \end{bmatrix}$$

columns 1 to 4 are replaced respectively by R in Δ to get Δ_i for i=1 to 4.

$$\theta_1 = a_1 Cosh2p_1 y + a_2 Sinh2p_1 y + a_3 Cosh2p_2 y + a_4 Sinh2p_2 y + a_5 Sinhp_2 y + a_6 Coshp_2 y + a_7 Sinhp_1 y + a_8 Coshp_1 y + a_9 Cosh(p_1+p_2)y + a_{10} Cosh(p_1 - p_2)y + a_{11} Sinh(p_1 + p_2)y + a_{12} Sinh(p_1 - p_2)y + a_{13} y^2 + E_1 y + E_2 \quad (3.1.13)$$

$$u_1 = A_1 Cosh2p_1 y + A_2 Sinh2p_1 y + A_3 Cosh2p_2 y + A_4 Sinh2p_2 y + A_5 Sinhp_2 y + A_6 Coshp_2 y + A_7 Sinhp_1 y + A_8 Coshp_1 y + A_9 Cosh(p_1+p_2)y + A_{10} Cosh(p_1 - p_2)y + A_{11} Sinh(p_1 + p_2)y + A_{12} Sinh(p_1 - p_2)y + A_{13} y^2 + A_{14} y + A_{15} \quad (3.1.14)$$

where A_i's are constants for i=1 to 15 shown in the Appendix.

Case (ii): Comparable porosity (i.e. $4k\ell^2 = 1$)

$$u_0 = (\bar{B}_1 + \bar{B}_2 y)\cosh p_3 y + (\bar{B}_3 + \bar{B}_4 y)\sinh p_3 y + \frac{1}{\ell^2} - \frac{m(1-y)}{2\ell^2}, \quad (3.1.15)$$

where $p_3 = \sqrt{\frac{1}{2k}}$, a real number,

the coefficients in Eq. (3.1.15) are computed using Cramer's rule i.e., $\bar{B}_j = \frac{\Delta_{1j}}{\Delta_1}$,

$$\Delta_1 = \begin{bmatrix} Chp_3 & Chp_3 & Shp_3 & Shp_3 \\ Chp_3 & -Chp_3 & -Shp_3 & Shp_3 \\ p_3^2 Chp_3 & 2p_3 Shp_3 + p_3^2 Chp_3 & p_3^2 Shp_3 & 2p_3 Chp_3 + p_3^2 Shp_3 \\ p_3^2 Chp_3 & -2p_3 Shp_3 - p_3^2 Chp_3 & -p_3^2 Shp_3 & 2p_3 Chp_3 + p_3^2 Shp_3 \end{bmatrix}$$

columns 1 to 4 are replaced respectively by R in Δ_1 to get Δ_{1j} for j=1 to 4.

$$\theta_1 = Z_{17}\ y^2\ Cosh2p_3 y + Z_{18}\ y^2 Sinh2p_3 y + Z_{19}\ y\ Cosh2p_3 y + Z_{20}\ y\ Sinh2p_3 y + Z_{21}\ Cosh2p_3 y + Z_{22}\ Sinh2p_3 y + Z_{23}\ y\ Coshp_3 y + Z_{24}\ y\ Sinhp_3 y + Z_{25}\ Coshp_3 y + Z_{26}\ Sinhp_3 y + \frac{Z_{10}}{2} y^2 + \frac{Z_8}{6} y^3 + \frac{Z_3}{12} y^4 + l_3 y + l_4. \quad (3.1.16)$$

Where Z_i's are constants for i=1 to 26 shown in the Appendix.

Case (iii): Dense porosity (i.e. $4k\ell^2 > 1$)

Kathmandu University
Journal of Science, Engineering and Technology

Siddalinga & Shashikala, Vol. 12, No. I, June, 2016, pp 49-62.

$$u_0 = \bar{C}_1 \cosh p_4 y + \bar{C}_2 \sinh p_4 y + \bar{C}_3 \cosh p_5 y + \bar{C}_4 \sinh p_5 y + \frac{1}{\ell^2} - \frac{m(1-y)}{2\ell^2}, \quad (3.1.17)$$

where $p_4 = \sqrt{\frac{1+\sqrt{1-4k\ell^2}}{2k}}$, $p_5 = \sqrt{\frac{1-\sqrt{1-4k\ell^2}}{2k}}$ are imaginary numbers,

the coefficients in Eq. (3.1.17) are computed using Cramer's rule i.e., $\bar{C}_i = \frac{\Delta_{2i}}{\Delta_2}$,

$$\Delta_2 = \begin{bmatrix} Chp_4 & Shp_4 & Chp_5 & Shp_5 \\ Chp_4 & -Shp_4 & Chp_5 & -Shp_5 \\ p_4^2 Chp_4 & p_4^2 Shp_4 & p_5^2 Chp_5 & p_5^2 Shp_5 \\ p_4^2 Chp_4 & -p_4^2 Shp_4 & p_5^2 Chp_5 & -p_5^2 Shp_5 \end{bmatrix}$$

columns 1 to 4 are replaced respectively by R in Δ_2 to get Δ_{2i} for i=1 to 4.

$$\theta_1 = a_1 Cosh2p_4 y + a_2 Sinh2p_4 y + a_3 Cosh2p_5 y + a_4 Sinh2p_5 y + a_5 Sinhp_5 y + a_6 Coshp_5 y + a_7 Sinhp_4 y + a_8 Coshp_4 y + a_9 Cosh(p_{4+}p_5) y + a_{10} Cosh(p_4 - p_5) y + a_{11} Sinh(p_4 + p_5) y + a_{12} Sinh(p_4 - p_5) y + a_{13} y^2 + E_1 y + E_2 \quad (3.1.18)$$

$$u_1 = A_1 Cosh2p_4 y + A_2 Sinh2p_4 y + A_3 Cosh2p_5 y + A_4 Sinh2p_5 y + A_5 Sinhp_5 y + A_6 Coshp_5 y + A_7 Sinhp_4 y + A_8 Coshp_4 y + A_9 Cosh(p_{4+}p_5) y + A_{10} Cosh(p_4 - p_5) y + A_{11} Sinh(p_4 + p_5) y + A_{12} Sinh(p_4 - p_5) y + A_{13} y^2 + A_{14} y + A_{15} \quad (3.1.19)$$

where A_i's are constants for i=1 to 15 shown in the Appendix.

2. Numerical Solution:

Analytical solution of Eqs. (2.8) – (2.9) using perturbation technique is valid only for the small values of the buoyancy parameter N. To know the validity of these solutions we solve them numerically using finite difference technique. All the derivatives are replaced by their central difference approximations of second order accuracy by dividing the region of interest into 80 mesh points of equal width of 0.025. The discretised form of Eqs. (2.8) and (2.9) are

$$u_{i+2} - \left(4 + \frac{h^2}{k}\right) u_{i+1} + \left(6 + \frac{2h^2}{k} + \frac{h^4 \sigma^2}{k}\right) u_i - \left(4 + \frac{h^2}{k}\right) u_{i-1} + u_{i-2} = \frac{h^4}{k} \theta_i \quad (3.2.1)$$

$$\theta_{i+2} - 2\theta_{i+1} + \theta_{i-1} + \frac{N}{4}(u_{i+1} + u_{i-1})^2 = 0 \quad (3.2.2)$$

Equations (3.2.1) and (3.2.2) are valid over the each grid point of the region and they give two implicit equations for u_i and θ_i, in-turn, they separately generate the system of algebraic equations for $u_{i+2}, u_{i+1}, u_i, u_{i-1}, u_{i-2}$ and $\theta_{i+1}, \theta_i, \theta_{i-1}$ resulting in a penta-diagonal coefficient matrix for u and a tri-diagonal coefficient matrix for θ. These equations are solved using the method of successive over relaxation (SOR) technique simultaneously at each mesh point till the required order of accuracy

Kathmandu University
Journal of Science, Engineering and Technology

Siddalinga & Shashikala, Vol. 12, No. I, June, 2016, pp 49-62.

of 10^{-8}. Analytical and numerical solutions of equations governing velocity are plotted graphically for sparse porosity, comparable porosity and dense porosity in Figs. 2 to 12, temperature profiles are plotted in Figs.13 to 15 and the results are discussed in section 5.

3. Skin Friction, Rate of Heat Transfer and Mass Flow Rate:

In many practical applications involving separation of flow it is advantage us to know the skin friction and the rate of heat transfer at the boundaries. These can be determined once we know the velocity and temperature distributions. The skin friction τ at the walls in the dimensionless form is

$$\tau = \left(\frac{du}{dy}\right)_{y=\pm 1} = \left(\frac{du_0}{dy}\right)_{y=\pm 1} + N\left(\frac{du_1}{dy}\right)_{y=\pm 1}. \tag{4.1}$$

Similarly, the rate of heat transfer between the fluid and the plate in the dimensionless form is,

$$q = \left(\frac{d\theta}{dy}\right)_{y=\pm 1} = \left(\frac{d\theta_0}{dy}\right)_{y=\pm 1} + N\left(\frac{d\theta_1}{dy}\right)_{y=\pm 1}. \tag{4.2}$$

Here $\frac{du}{dy}$ and $\frac{d\theta}{dy}$ are computed numerically using Newton's interpolation formula for derivatives.

If M_f denotes the mass flow rate per unit channel width in the presence of dissipation, then

$$M_f = \int_{-1}^{1} u\, dy. \tag{4.3}$$

Mass flow rate given by Eq. (4.3) is computed numerically Simpson's rule for numerical integration. Results obtained from Eqs. (4.1) - (4.3) are depicted graphically in Figs. (16) to (24) respectively for different parameters and the conclusions are drawn in the section 5.

RESULTS AND DISCUSSIONS

The theory of couple stress fluid due to Stokes is used to formulate a set of boundary layer equations for the flow of an incompressible, couple stress fluid in the presence of a uniform transverse magnetic field in a vertical porous channel. In the preceding section analytical and numerical solutions are obtained.

Effect of magnetic field on the flow is depicted in Fig.2 for the case of sparse porosity, in Fig.3 for the case of comparable porosity and in Fig.4 for dense porosity by keeping other parameters constant. It is observed that as the Hartmann number M is increases the velocity decreases in all the three cases. However, for comparable porosity case the magnetic field is operative even for large values of M. M=0 represent the case of absence of magnetic field.

Kathmandu University
Journal of Science, Engineering and Technology

Siddalinga & Shashikala, Vol. 12, No. I, June, 2016, pp 49-62.

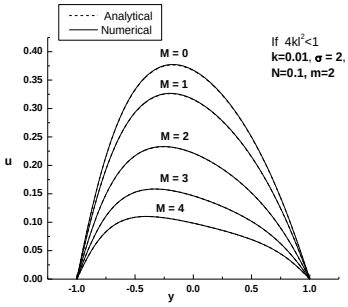

Figure 2: Velocity Profiles for different values of M for sparse porosity

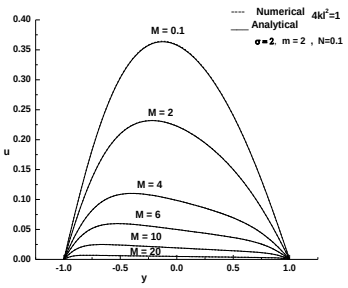

Figure 3: Velocity Profiles for different values of M for comparable porosity

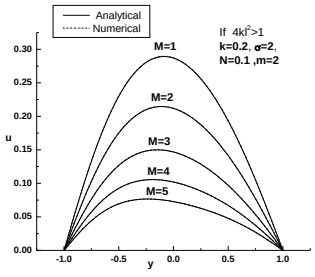

Figure 4: Velocity Profiles for different values of M for dense porosity

Effect of temperature parameter m on flow is depicted in Fig.5 for sparse porosity, in Fig.6 for comparable porosity and in Fig.7 for dense porosity. m=0 implies that the plates are maintained at constant temperature, m=1,2 represent the heating of plate at y=-1, hence the velocity increases with increase in m due to the increase in convection. When m = -1, -2 indicate still the heating is present and hence there will be flow reversal and separation occurs at y = 0.

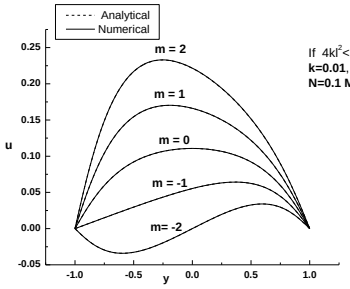

Figure 5: Velocity Profiles for different values of m for sparse porosity

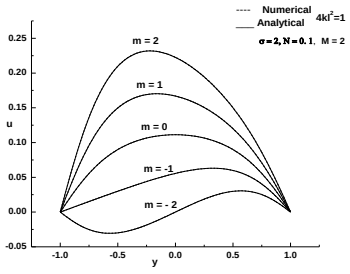

Figure 6: Velocity Profiles for different values of m for comparable porosity

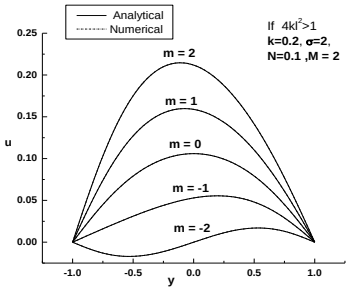

Figure 7: Velocity Profiles for different values of m for dense porosity

Effect of porous parameter σ on flow is depicted in Fig.8 for sparse porosity, in Fig.9 for comparable porosity and in Fig. 10 for dense porosity. As σ increases, the velocity decreases because of dampening effect of Darcy force. For small values of σ the velocity is high in the sparse porosity case, whereas for the case of large values of σ the velocities are all in the same range.

Kathmandu University
Journal of Science, Engineering and Technology

Siddalinga & Shashikala, Vol. 12, No. I, June, 2016, pp 49-62.

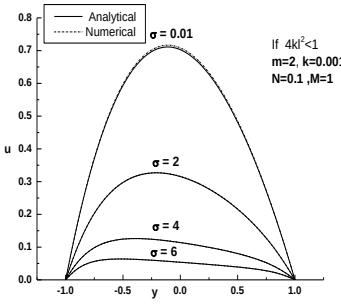

Figure 8: Velocity Profiles for different values of σ for sparse porosity

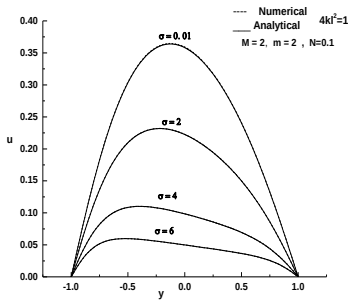

Figure 9: Velocity Profiles for different values of σ for comparable porosity

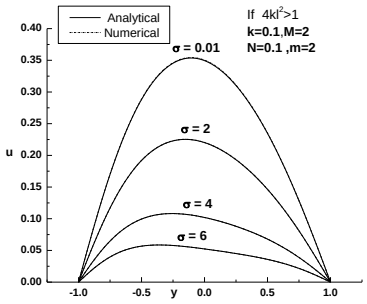

Figure 10: Velocity Profiles for different values of σ for dense porosity

Figures 11 and 12 represent the variation of velocity for varying couple stress parameter k for sparse and dense porosity cases respectively. The case of comparable porosity is not discussed, since to make $4k\ell^2 = 1$we have taken k as the parameter. As, k increases the velocity decreases in both the cases. In the case of sparse porosity k is operative in a very narrow region, whereas, for dense porosity it is operative for large value of k. Figs.2 – 12 clearly show that the analytical and numerical solutions agree well.

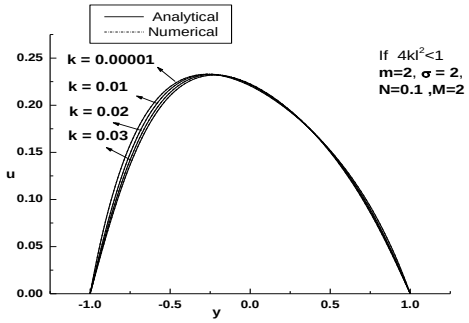

Figure 11: Velocity Profiles for different values of k for sparse porosity

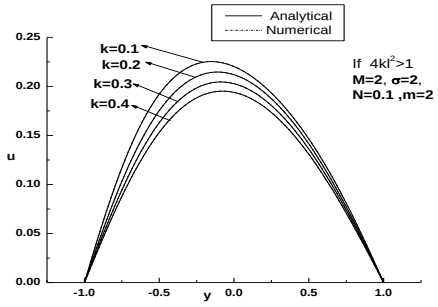

Figure 12: Velocity Profiles for different values of k for dense porosity

Variations of temperature for the case of sparse porosity are depicted in Figs. 13 – 14. In Fig.13 we notice that as the porous parameter increases the temperature decreases very narrowly, implying that Darcy velocity has minimum influence on temperature distribution. Figure 14 represents the variation of temperature parameter. It is observed that as the temperature parameter m increases temperature also increases. Analogous results are observed for comparable and dense porosity cases; hence they are omitted.

Results reported above are valid for small values of buoyancy parameter N. The numerical solution for temperature distribution for wide range of values of N is presented in Fig. 15. From this figure it is clear that as N increases temperature also increases as expected.

Kathmandu University
Journal of Science, Engineering and Technology

Siddalinga & Shashikala, Vol. 12, No. I, June, 2016, pp 49-62.

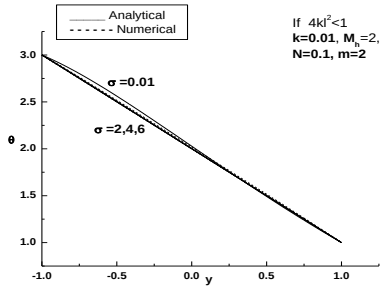

Figure 13: Temperature Profiles for different values of σ

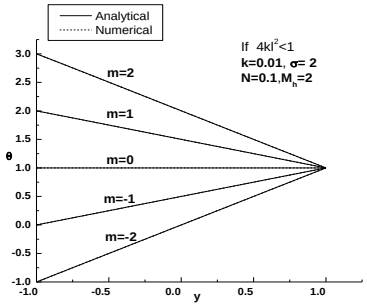

Figure 14: Temperature Profiles for different values of m

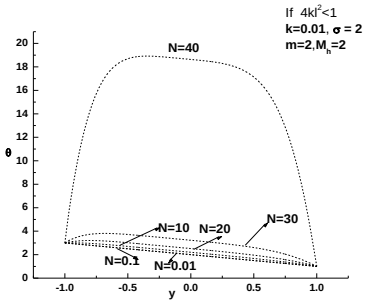

Figure 15: Temperature Profiles for different values of N

It is known from the literature that Skin friction τ, Rate of heat transfer q and Mass flow rate M_f increase with increase in buoyancy parameter N due to transfer of more heat. Hence, in this paper an attention is given to other parameters namely couple stress parameter k, heat transfer coefficient m and Hartmann number M on τ,q and M_f.

The plot of Skin friction τ at the cold plate versus the porous parameter σ for different values of k, m and M are shown in Figs.16 – 18. From the graphs it is clear that as the parameters are increased the skin friction decreases considerably.

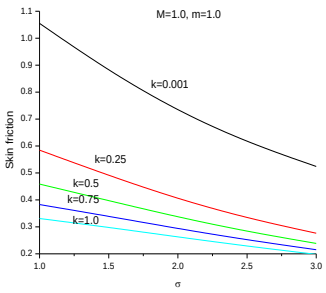

Figure 16: Skin friction profiles for different values of k

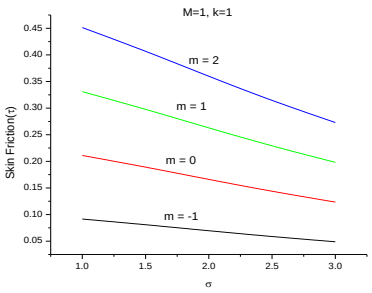

Figure 17: Skin friction profiles for different values of m

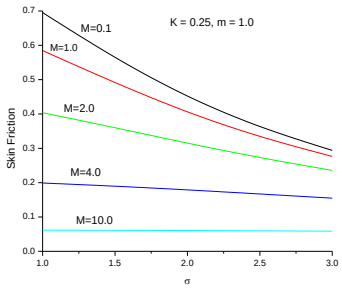

Figure 18: Skin friction profiles for different values of M

Figures 19-21 represent the graph of rate of heat transfer q versus the porous parameter σ for varying k, m and M respectively. It is observed that as we increase the parameters k, q and m, the rate of heat transfer, q decreases. Thus increase in parameter decreases the rate of heat transfer.

Kathmandu University
Journal of Science, Engineering and Technology

Siddalinga & Shashikala, Vol. 12, No. I, June, 2016, pp 49-62.

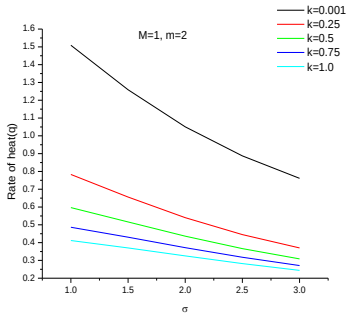

Figure 19: Rate of heat transfer profiles for different values of k

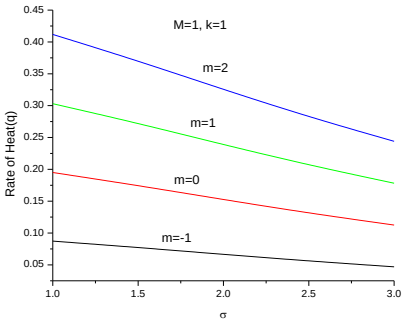

Figure 20: Rate of heat transfer profiles for different values of m

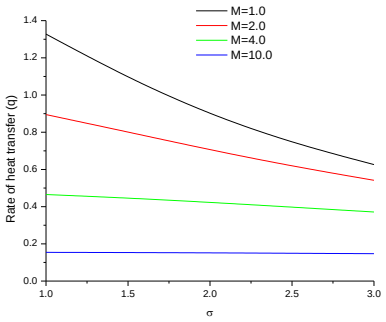

Figure 21: Rate of heat transfer profiles for different values of M

Mass flow rate M_f versus the porous parameter σ are plotted in Figs.22-24, the effect of increasing k,m and M decrease the mass flow rate.

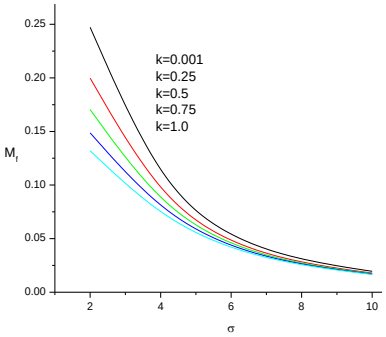

Figure 22: Mass flow rate profiles for different values of k

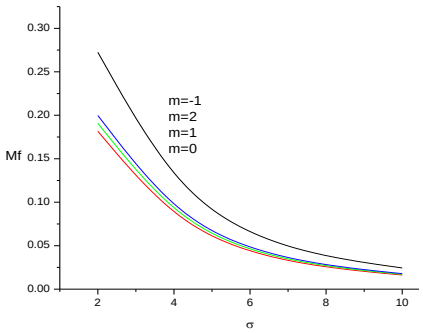

Figure 23: Mass flow rate profiles for different values of m

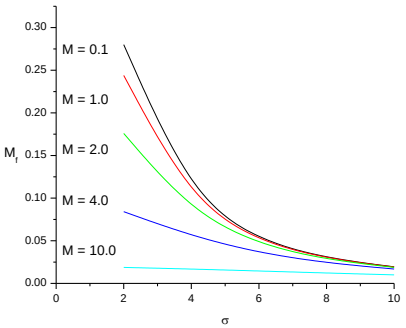

Figure 24: Mass flow rate profiles for different values of M

Thus τ ,q and M_f decrease as the parameters k, m and M increase.

CONCLUSIONS

We consider the fully developed convective flow of a couple stress fluid through porous media in a vertical channel with an external constraint of applied magnetic field. Governing equations are expressed in non-dimensional form and then solved analytically by perturbation technique and numerically by finite difference technique. Features of the flow characteristics are analysed by plotting graphs with detailed discussion. Summary of main finding are as follows:

i. Fluid velocity is a function of Hartmann number, temperature parameter, porous parameter and couple stress parameter. Fluid velocity varies directly with temperature parameter and inversely with the other parameters.

ii. Fluid temperature is a function of a porous parameter, temperature parameter and buoyancy parameter. Temperature of the fluid varies inversely with the porous parameter and directly with the other parameters.

Siddalinga & Shashikala, Vol. 12, No. I, June, 2016, pp 49-62.

iii. The flow characteristics namely Skin friction, Rate of heat transfer and Mass flow rate are functions of the parameters couple stress parameter, temperature parameter and Hartmann number. All the flow characteristics vary inversely with the parameters.

Hence with the proper choice of the parameters it is possible to control the fluid velocity, temperature and other flow characteristics.

ACKNOWLEDGEMENT

We thank the referee for the valuable comments.

REFERENCES

[1] Elenbaas, W, Heat dissipation of parallel plates by free convection, *Physica Col.IX*, (1942) 1(1).

[2] Bodoia J R & Osterle J F, The development of free convection between heated vertical plates, *ASME Journal of Heat Transfer*, (1962) 84(1): 40.

[3] Aung W, Fletcher L S & Sernas V, Developing laminar free convection between vertical flat plates with asymmetric heating, *Int. J. Heat Mass Transfer*, (1972) 15: 2293.

[4] Aero E L, Bullygin A N & Kuvshinskii E V, Asymmetric Hydrodynamics, *Appl. Math. Mech.*, (1963) 333: 29.

[5] Eringen A C, Simple Micro-fluids, *Int. J. Engng. Sci.* (1964) 2: 205.

[6] Stokes V K, Couple stresses in fluid, *Physics of Fluids*, (1966) 9(9): 1709.

[7] Umavathi J C & Malashetty M S, Oberbeck convection flow of a couple stress fluid through a vertical porous stratum, *Int. J. Nonlinear Mech.*, (1999) 34: 1037.

[8] Al-Rashdan M, Fayyad S M & Frihat M, Heat and mass fully-developed natural-convective viscous flow with chemical reaction in porous medium, *Adv. Theor. Appl. Mech*, (2012) 5(3): 93.

[9] Tomer N S, Phool S & Manoj K, Effect of variable viscosity on convective heat transfer along an inclined plate embedded in porous medium with an applied magnetic field, *World Academy of Science and Technology*, (2011) 51: 770.

[10] Rudraiah N, Byalakere S & Shashikala S, Non-linear Oberbeck-electroconvection in a poorly conducting fluid through a vertical channel in the presence of an electric field, *Int. J of Non-Linear Mechanics*, (2007) 42(3): 403.

[11] Srinivasacharya D & Kaladhar K, Natural convection flow of a couple stress fluid between two vertical parallel plates with Hall and ion-slip effects, *Acta Mech. Sin.*, (2012) 28(1): 41.

Kathmandu University
Journal of Science, Engineering and Technology

Siddalinga & Shashikala, Vol. 12, No. I, June, 2016, pp 49-62.

[12] Rudraiah N, Rajaprakash B & Nagaraju, Non-linear oberbeck convection in chiral fluid through a vertical permeable channel in the presence of a transverse magnetic field, *Journal of Applied Fluid Mechanics*, (2014) 7(1): 1735.

Appendix:

Case 1:

$A_1 = \frac{a_1}{16Kp_1^4 - 4p_1^2 + l^2}, A_2 = \frac{a_2}{16Kp_1^4 - 4p_1^2 + l^2}, A_3 = \frac{a_3}{16Kp_1^4 - 4p_1^2 + l^2},$

$A_4 = \frac{a_4}{16Kp_1^4 - 4p_1^2 + l^2}, A_5 = \frac{a_5}{Kp_2^4 - p_2^2 + l^2}, A_6 = \frac{a_6}{Kp_2^4 - p_2^2 + l^2}, A_7 = \frac{a_7}{Kp_1^4 - p_1^2 + l^2}, A_8 = \frac{a_8}{Kp_1^4 - p_1^2 + l^2}, A_9 = \frac{a_9}{K(p_1+p_2)^4 - (p_1+p_2)^2 + l^2}, A_{10} = \frac{a_{10}}{K(p_1-p_2)^4 - (p_1-p_2)^2 + l^2},$

$A_{11} = \frac{a_{11}}{K(p_1+p_2)^4 - (p_1+p_2)^2 + l^2}, A_{12} = \frac{a_{12}}{K(p_1-p_2)^4 - (p_1-p_2)^2 + l^2}, A_{13} = \frac{a_{13}}{l^2}, A_{14} = \frac{E_1}{l^2}$

$A_{15} = \frac{2a_{13}}{l^4} + \frac{E_2}{l^2},$

Case 2:

$Z_1 = -B_1 p_3 - B_4, Z_2 = -B_3 p_3 - B_2, Z_3 = -B_2 p_3, Z_4 = -B_4 p_3, l_2 = -\frac{m}{2l^2}, Z_5 = \frac{Z_1^2 + Z_2^2}{2}, Z_6 = \frac{Z_3^2 + Z_4^2}{2}, Z_7 = Z_1 Z_3 + Z_2 Z_4, Z_8 = Z_1 Z_3 - Z_2 Z_4,$

$Z_9 = \frac{Z_3^2 + Z_4^2}{2}, Z_{10} = \frac{Z_1^2 - Z_2^2 + 2l_2^2}{2}, Z_{11} = \frac{Z_7}{2p_3} - \frac{2Z_3 Z_4}{4p_3^2},$

$Z_{12} = -\frac{2Z_6}{4p_3^2} + \frac{Z_1 Z_4}{2p_3} + \frac{Z_2 Z_3}{2p_3}, Z_{13} = \frac{2Z_6}{8p_3^3} - \frac{Z_1 Z_4}{4p_3^2} - \frac{Z_2 Z_3}{4p_3^2} + \frac{Z_5}{2p_3},$

$Z_{14} = -\frac{Z_7}{4p_3^2} + \frac{2Z_3 Z_4}{8p_3^3} + \frac{Z_2 Z_1}{2p_3}, Z_{15} = \frac{2Z_2 l_2}{p_3} - \frac{2Z_3 l_2}{p_3^2}, Z_{16} = \frac{2Z_1 l_2}{p_3} - \frac{2Z_4 l_2}{p_3^2}, Z_{17} = \frac{Z_6}{4p_3^2}, Z_{18} = \frac{Z_2 Z_3}{4p_3^2}, Z_{19} = \frac{Z_{11}}{2p_3} - \frac{Z_3 Z_2}{4p_3^3}, Z_{19} = \frac{Z_{12}}{2p_3} - \frac{Z_6}{8p_3^3}, Z_{21} = \frac{Z_6}{8p_3^4} + \frac{Z_{13}}{2p_3} - \frac{Z_{12}}{4p_3^2}, Z_{22} = \frac{Z_3 Z_2}{8p_3^4} - \frac{Z_{11}}{4p_3^2} + \frac{Z_{14}}{2p_3}, Z_{23} = \frac{2Z_4 l_2}{p_3^2}, Z_{24} = \frac{2Z_3 l_2}{p_3^2}, Z_{25} = -\frac{2Z_3 l_2}{p_3^3} + \frac{Z_{15}}{p_3}, Z_{26} = -\frac{2Z_4 l_2}{p_3^3} + \frac{Z_{16}}{p_3},$